


## Regulatory network for *FOREVER YOUNG FLOWER*-like genes in regulating *Arabidopsis* flower senescence and abscission

Wei-Han Chen<sup>1,3</sup>, Pei-Tzu Lin<sup>1,3</sup>, Wei-Han Hsu<sup>1,3</sup>, Hsing-Fun Hsu<sup>1</sup>, Ya-Chun Li<sup>1</sup>, Chin-Wei Tsao<sup>1</sup>, Mao-Cheng Hsu<sup>1</sup>, Wan-Ting Mao<sup>1</sup> & Chang-Hsien Yang<sup>1,2</sup>  [✉](mailto:chyang@dragon.nchu.edu.tw)

*FOREVER YOUNG FLOWER* (*FYF*) has been reported to play an important role in regulating flower senescence/abscission. Here, we functionally analyzed five *Arabidopsis* *FYF*-like genes, two in the *FYF* subgroup (*FYL1/AGL71* and *FYL2/AGL72*) and three in the *SOC1* subgroup (*SOC1/AGL20*, *AGL19*, and *AGL14/XAL2*), and showed their involvement in the regulation of flower senescence and/or abscission. We demonstrated that in *FYF* subgroup, *FYF* has both functions in suppressing flower senescence and abscission, *FYL1* only suppresses flower abscission and *FYL2* has been converted as an activator to promote flower senescence. In *SOC1* subgroup, *AGL19/AGL14/SOC1* have only one function in suppressing flower senescence. We also found that *FYF*-like proteins can form heterotetrameric complexes with different combinations of A/E functional proteins (such as *AGL6* and *SEP1*) and *AGL15/18*-like proteins to perform their functions. These findings greatly expand the current knowledge behind the multifunctional evolution of *FYF*-like genes and uncover their regulatory network in plants.

<sup>1</sup>Institute of Biotechnology, National Chung Hsing University, Taichung, Taiwan 40227, ROC. <sup>2</sup>Advanced Plant Biotechnology Center, National Chung Hsing University, Taichung, Taiwan 40227, ROC. <sup>3</sup>These authors contributed equally: Wei-Han Chen, Pei-Tzu Lin, Wei-Han Hsu. ✉email: [chyang@dragon.nchu.edu.tw](mailto:chyang@dragon.nchu.edu.tw)

We have previously reported that *Arabidopsis* FOREVER YOUNG FLOWER (*FYF*) specifically regulates flower organ senescence and abscission by suppressing the downstream genes of ethylene signaling *EDF1/2/3/4* and abscission-associated genes *BOP1/2* and *IDA*<sup>1,2</sup>. Conserved functions in regulating flower organ senescence and abscission have been reported for *FYF* orthologs identified in different species of orchids<sup>3–5</sup>. Based on sequence homology and phylogenetic analysis, six putative closely related *FYF*-like genes could be subjected to two subgroups: (1) the *FYF* group composed of *FYF*, *AGL71*, and *AGL72* and (2) the *SOC1* group composed of *AGL20* (*SOC1*), *AGL19*, and *AGL14* (*XAL2*) in the *Arabidopsis* genome<sup>6</sup>.

It has been reported that additional new genes could be generated in the genome through gene duplication, which was thought to play an important role in organisms during evolution<sup>7–9</sup>. Phylogenetic analysis revealed that three duplication events from an *FYF*-like ancestor may have occurred (two within subgroups) to generate six *Arabidopsis* *FYF*-like genes<sup>6</sup>. Functional analysis indicated that the majority of the duplicate *FYF*-like gene pairs (*FYF/AGL71/AGL72/SOC1/AGL19/AGL14*) may retain overlap of the original ancestral function, such as the regulation of flowering time<sup>10–23</sup>, or have specific subsets of the original ancestral function, such as the regulation of root<sup>24,25</sup> and ovule<sup>26</sup> development as seen for *AGL14* (*XAL2*), which was described as subfunctionalization<sup>9,27–30</sup>. Although different putative functions were uncovered for these *Arabidopsis* *FYF*-like genes, exploration of the function in regulating flower organ senescence and abscission was investigated for only the *FYF* gene and has never been reported for other five *Arabidopsis* *FYF*-like genes. It is therefore not clear whether the *FYF* gene evolved to have this unique function in regulating flower organ senescence and abscission from its ancestor or whether some of the other *FYF*-like genes also harbored this function during evolution. To uncover these questions, we comprehensively functionally characterized all putative *Arabidopsis* *FYF*-like genes for their involvement in regulating flower organ senescence and abscission. Furthermore, we used a FRET-based strategy to investigate the possible heterotetrameric protein complexes formed by the interactions of *FYF*-like and other MADS box proteins to further verify the regulatory networks for these duplicate *FYF*-like gene pairs in *Arabidopsis*.

Here, we show that all other five *Arabidopsis* *FYF*-like genes have a function in regulating flower senescence and/or abscission similar to *FYF*. In this work, we also found that *FYF*-like proteins can interact with different combinations of A/E functional proteins (such as *AGL6* and *SEP1*) and *AGL15/18*-like proteins (such as *AGL15/18*) to form heterotetrameric complexes in regulating flower senescence and abscission.

## Results

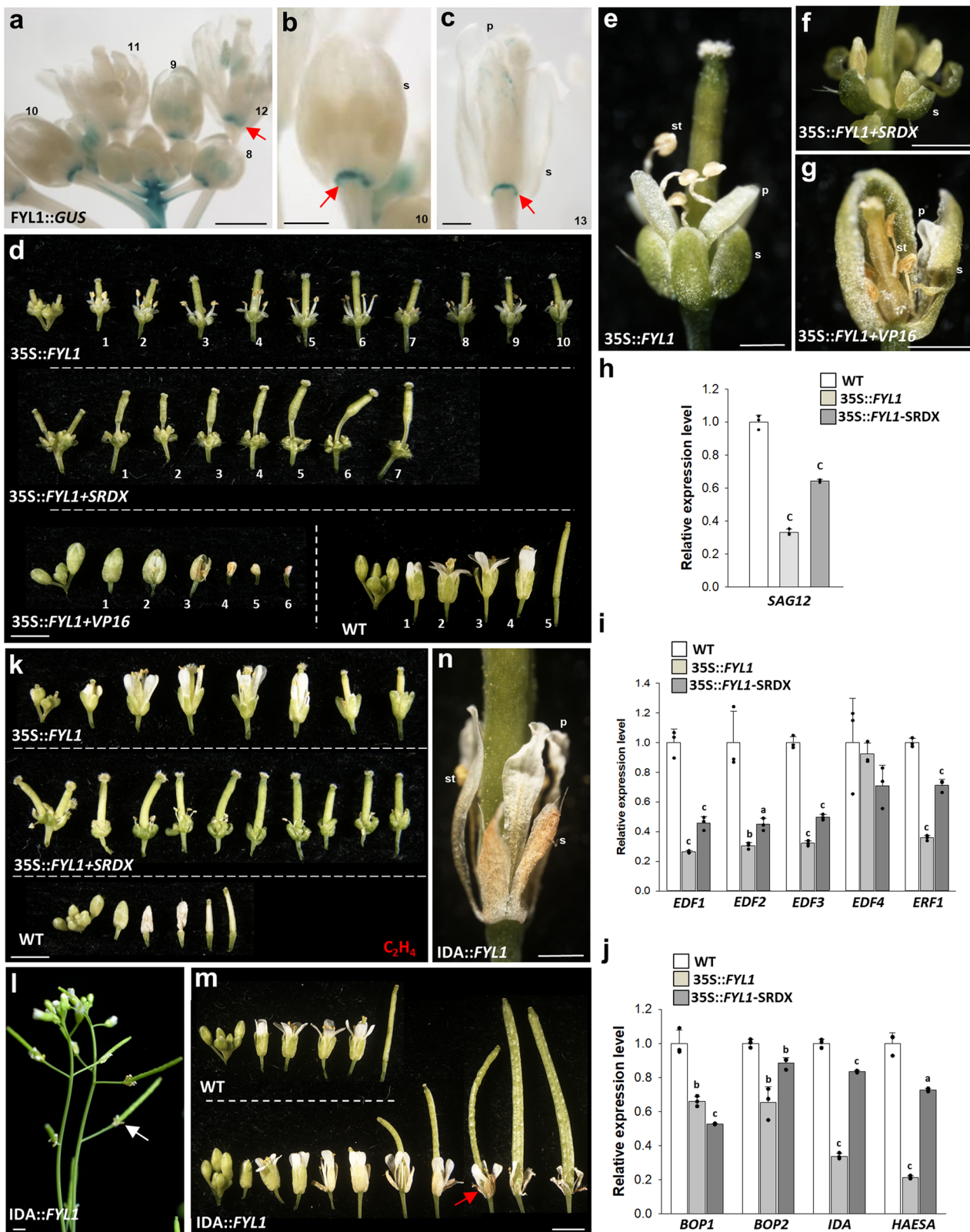
**Characterization of two *FYF* closely related genes, *FYL1* and *FYL2*.** Two *Arabidopsis thaliana* MADS box genes, known to be closely related to *FYF* (AT5G62165), named *FYF-like 1, 2* (*FYL1/AGL71*, *FYL2/AGL72*), in the *FYF* group were analyzed. *FYL1* (AT5G51870) encodes a protein containing 219 amino acids that showed 40.3% identity to *FYF*, with 86.2% (50/58) of the amino acids being identical in the MADS box domain (Supplementary Fig. 1). *FYL2* (AT5G51860) encodes a protein containing 202 amino acids that showed 43.7 and 65% identity to *FYF* and *FYL1*, respectively, with 86.2% (50/58) and 94.8% (55/58) of the amino acids being identical in the MADS box domain (Supplementary Fig. 1), respectively. The amino acid identity and the phylogenetic tree relationship<sup>6</sup> indicated that *FYL1* was more closely related to *FYL2* than to *FYF* (Supplementary Fig. 2).

**The distinct expression patterns of *FYL1* and *FYL2*.** To investigate the expression patterns of the *FYL1* and *FYL2* genes, *FYL1/2* expression was further analyzed in flowers at different developmental stages. The results indicated that higher *FYL1/2* expression was observed during early flower development (before stage 9) than during late developmental stages (after stage 12) (Supplementary Fig. 3a, b), which was similar to the spatial and temporal expression pattern of *FYF* during flower development (Supplementary Fig. 3c)<sup>1</sup>. When *FYL1::GUS* and *FYL2::GUS* constructs were generated and transformed into *Arabidopsis*, *GUS* staining was exclusively detected in the abscission zone (AZ) of the sepals/petals of *FYL1::GUS* flowers (Fig. 1a–c) and shows a more extended pattern in the sepals/petals of *FYL2::GUS* flowers (Fig. 2a–d). Further RT-qPCR analysis indicated that *FYL1* expression was highly detected whereas *FYL2* expression was almost undetectable in the AZ (Supplementary Fig. 3d). This result is interesting since *GUS* staining was detected in both sepals/petals and in the abscission zones of *FYF::GUS* flowers<sup>1</sup>, suggesting that *FYL1* and *FYL2* might have different subfunctions of *FYF* in regulating flower senescence and abscission.

***FYL1* delayed flower senescence and abscission once ectopically expressed in transgenic *Arabidopsis* plants.** To investigate function correlated to the expression pattern of *FYL1*, 35S::*FYL1*, 35S::*FYL1*+*SRDX* (containing a suppression motif), and 35S::*FYL1*-*DR*+*VP16* (containing an activation *VP16*-*AD*) were transformed into *Arabidopsis*. The 35S::*FYL1* plants showed a delay in both flower senescence and abscission (Fig. 1d, top and 1e), similar to what was observed in 35S::*FYF* plants<sup>1</sup>. Furthermore, enhancement of the delay of flower senescence/abscission was observed in 35S::*FYL1*+*SRDX* transgenic plants (Fig. 1d, middle and 1f), and an opposite promotion of flower senescence/abscission was produced in 35S::*FYL1*-*DR*+*VP16* transgenic plants (Fig. 1d, bottom left and 1g), suggesting that *FYL1* should act as a repressor in suppressing flower senescence/abscission, similar to *FYF*. Once it has been converted into an activator, *FYL1*-*DR*+*VP16*, an opposite dominant negative mutant phenotype will be observed. We also found that the expression of the senescence-associated gene *SAG12*, downstream genes in ethylene signaling *EDF1-3*, and *ERF1* and abscission-associated genes *BOP1/2*, *IDA*, and *HAESA* were all downregulated in 35S::*FYL1* and 35S::*FYL1*+*SRDX* plants (Fig. 1h–j). In addition, 35S::*FYL1* and 35S::*FYL1*+*SRDX* flowers were insensitive to ethylene treatment (Fig. 1k). Our data suggest that *FYL1* could have a prominent role like *FYF* in controlling floral senescence/abscission once ectopically expressed in *Arabidopsis* flowers. However, *FYL1* should only have a partial role in controlling floral abscission in real life since its expression was restricted to the abscission zone (AZ) of the sepals/petals of flowers (Fig. 1a–c and Supplementary Fig. 3d).

To further confirm the relationship between *FYL1* and sepal/petal abscission, the *FYL1* gene driven by the *IDA* promoter (*IDA::FYL1*) was transformed into *Arabidopsis*. A clear delay in the abscission of the perianth organs was observed in *IDA::FYL1* flowers (Fig. 1l–n). However, senescence of the perianth normally occurred from positions 4–5 in these flowers that were not abscised in the *IDA::FYL1* transgenic plants (Fig. 1l–n). This phenotype was very similar to what has been observed in *ida* mutants<sup>31</sup> and *IDA::FYF* plants<sup>1</sup>; thus, the result supported the role of *FYL1* as a suppressor and its function together with *FYF* in suppressing *IDA* and sepal/petal abscission.

***FYL2* promoted flower senescence and abscission when ectopically expressed in transgenic *Arabidopsis* plants.** Similar to *FYL1*, 35S::*FYL2*, 35S::*FYL2*+*SRDX*, and 35S::*FYL2*-*DR*+*VP16*



*Arabidopsis* were generated. 35S::FYL2 plants surprisingly showed promotion of both flower senescence and abscission (Fig. 2e, first row and 2f). A similar promotion of flower senescence/abscission was observed in 35S::FYL2-DR+VP16 transgenic plants (Fig. 2e, third row and 2h), and an opposite delay of flower senescence/abscission was produced in 35S::FYL2+SRDX transgenic plants (Fig. 2e, second row and 2g), suggesting that FYL2 should act as

an activator in promoting flower senescence/abscission, in contrast to FYF and FYL1. We also found that the expression of *EDF1-4*, *ERF1*, *BOP1/2*, *IDA*, and *HAESA* were all downregulated in 35S::FYL2+SRDX plants (Fig. 2i-k). By contrast, *SAG12*, *EDF1-4*, *ERF1*, *IDA*, and *HAESA* were all upregulated in 35S::FYL2 and 35S::FYL2-DR+VP16 transgenic plants (Supplementary Fig. 4). In addition, 35S::FYL2+SRDX flowers were

**Fig. 1 Characterization of the *FYL1* gene through transgenic plants and gene expression analysis in *Arabidopsis*.** **a** GUS was strongly stained in the AZ (arrowed) of floral buds and mature flowers of *FYL1::GUS Arabidopsis*. The numbers indicate the different developmental stages of *Arabidopsis* flowers. Bar = 1 mm. Magnified view of stage 10 (**b**) and 13 (**c**) *FYL1::GUS* flowers. GUS was only strongly stained in the AZ (arrowed). s: sepal, p: petal. Bars = 0.5 mm. **d** Flowers along the inflorescences of *35S::FYL1* (first row), *35S::FYL1+SRDX* (second row) and *35S::FYL1+VP16* (third row, left) and wild-type (WT) (third row, right) plants. The numbers indicate the positions of the flowers. Bar = 1.5 mm. Magnified view of the delayed senescent *35S::FYL1* (**e**), *35S::FYL1+SRDX* (**f**) and early senescent *35S::FYL1+VP16* (**g**) flowers. s: sepal, p: petal, st: stamen. Bars = 0.5 mm. Detection of *SAG12* (**h**), *EDF1-4* and *ERF1* (**i**) and *BOP1/2*, *IDA* and *HAESA* (**j**) expression in *35S::FYL1* and *35S::FYL1+SRDX Arabidopsis*. Error bars show  $\pm$  SD.  $n = 3$  biologically independent samples. The expression of each gene in the transgenic plants is given relative to that of the wild-type plant, which was set at 1. The letter "a", "b" and "c" indicates significant difference from the wild-type (WT) value (a:  $P < 0.05$ , b:  $P < 0.01$ , and c:  $P < 0.001$ ). The two-sided Student's *t*-test was used. **k** Flowers along the inflorescence of *35S::FYL1* (first row), *35S::FYL1 + SRDX* (second row), and wild-type (third row) plants after exposure to ethylene. Bar = 2 mm. Inflorescence of *IDA::FYL1* plants (**l**) and flowers along the inflorescence (**m**) of *IDA::FYL1* (bottom) and wild-type (WT, top) plants. The flower organs (arrowed) remained on the *IDA::FYL1* flower and siliques. Bars = 2 mm. **n** Magnified view of an *IDA::FYL1* flower with a senescent but not abscised phenotype from (**m**). s: sepal, p: petal, st: stamen. Bar = 0.5 mm.

insensitive to ethylene treatment (Fig. 2l). This result suggested that *FYL2* should function opposite to *FYF* and could have the same role as *FYF* once it is converted into a repressor as *FYL2+SRDX*, and a dominant negative mutant phenotype in suppressing floral senescence/abscission will be observed. However, *FYL2* should only have an opposite role to *FYF* in controlling floral senescence in real life since its expression was specifically in the sepals/petals of flowers (Fig. 2a–d).

To further confirm the relationship between *FYL2* and *FYF* in regulating sepal/petal senescence, *35S::FYF* and *35S::FYL2* were doubly transformed into *Arabidopsis*, and plants ectopically expressing *FYF* and *FYL2* were generated simultaneously. A clear wild-type-like phenotype by senescence and abscission of the perianth organs at approximately positions 3–4 was observed in the *35S::FYF/35S::FYL2* flowers (Fig. 2m, right), which was earlier than that in the *35S::FYF* flowers (Fig. 2m, left) and later than that in the *35S::FYL2* flowers (Fig. 2e, first row). This *35S::FYF/35S::FYL2* intermediate phenotype between *35S::FYF* and *35S::FYL2* clearly indicated an antagonistic relationship between *FYF* and *FYL2*. Thus, the results supported a role for *FYL2* as an activator with a function antagonistic to part of the *FYF* function in controlling senescence of the sepal/petal.

**FYF can interact with AGL6 and SEP1 in regulating flower abscission/senescence.** To investigate which proteins could possibly interact with *FYF* to form a complex in regulating flower organ abscission and senescence, two potential candidates, *AGL6* and *SEP1*, which have been reported to be able to interact with *FYF* through yeast two-hybrid screen<sup>32</sup>, were identified. It is important to determine whether the spatial and temporal expression patterns of the *AGL6* and *SEP1* genes were correlated with *FYF*. Based on the *AGL6::GUS* assay, *AGL6* expression could be detected in the basal parts and abscission zone of the floral organs during floral development (Supplementary Fig. 5a–c)<sup>33</sup> and was detected to be more abundant in wild-type flowers before (BP) than after (AP) pollination (Supplementary Fig. 5d), which overlapped with the expression pattern of *FYF*. *SEP1* has been reported to be expressed in all four whorls of flower organs, is more abundant during early morphological differentiation than in mature flowers, and was not reported in the abscission zone during floral development<sup>34,35</sup>. These results suggested that *FYF* might interact with *AGL6* to form a complex in regulating sepal/petal abscission. In addition, *FYF* can interact separately with *SEP1* and *AGL6* to form a complex in regulating sepal/petal senescence.

We further performed FRET analyses by using *FYF*-CFP and *AGL6/SEP1*-YFP to observe physical interactions of *FYF* and *AGL6/SEP1* protein complexes in tobacco cells<sup>36</sup>. The results confirmed that *FYF/AGL6* formed heterodimers with high efficiency in the nucleus (Fig. 2n, column 1, Fig. 3a). The same

result was observed for *FYF/SEP1* (Fig. 2o, column 1). These results suggested that *FYF* is able to interact with *AGL6* and *SEP1* to form complexes in regulating flower senescence and/or abscission.

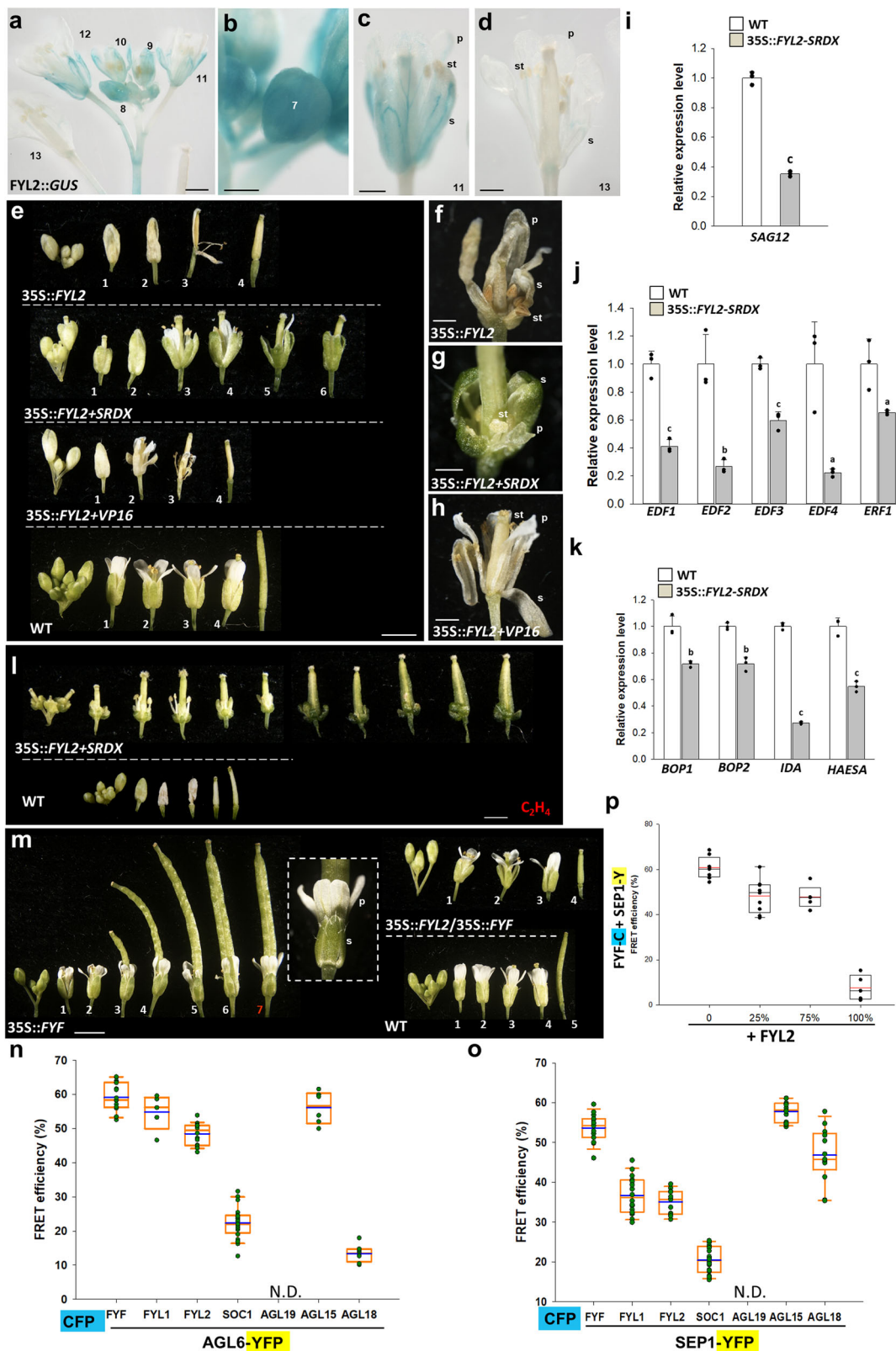
#### **FYL1 can interact with AGL6 in regulating flower abscission.**

To further investigate whether *FYL1* could also interact with proteins similar to *FYF* in regulating flower organ abscission, FRET analyses were performed. When *FYL1*-CFP and *AGL6/SEP1*-YFP were used to observe the physical interactions of *FYL1* and *AGL6/SEP1*, *FYL1/AGL6* can form heterodimers with similar efficiency to *FYF/AGL6* in the nucleus of tobacco cells (Fig. 2n, column 2, Fig. 3b). However, the efficiency for the formation of *FYL1/SEP1* (Fig. 2o, column 2) was clearly lower than that for *FYF/SEP1* (Fig. 2o, column 1). These results suggested that *FYL1* is able to interact with *AGL6* in a more stable manner than with *SEP1* to form complexes. Since *FYL1* was only expressed in the AZ of the sepals/petals and could only regulate flower organ abscission, it is reasonable to believe that *FYL1* can only physically interact with *AGL6* in the AZ to regulate abscission of the sepals/petals. Although they can interact, the *FYL1/SEP1* complex should not exist during *Arabidopsis* flower development since these two genes have no overlapping expression pattern.

The ability of *AGL6* to interact with *FYF* and *FYL1* to form complexes reveals that its function should be related to *FYF/AGL6*. This assumption was further supported by the result that a similar delay in the flower senescence/abscission phenotype (Supplementary Fig. 5e–i) and downregulation of *EDF1*, *BOP1/2*, *IDA*, and *HAESA* (Supplementary Fig. 5j, k) were observed in *35S::AGL6+SRDX* plants. This result revealed that *FYF/AGL6* can interact with *AGL6* to target similar downstream genes once expressed in the same places.

#### **FYF and FYL1 can interact with AGL6/AGL6 and AGL15 proteins to form stable heterotetrameric abscission complexes.**

Based on the floral quartet model in which plant MADS-box proteins function as higher-order tetrameric complexes<sup>37</sup>, we hypothesized that *FYF-AGL6* heterodimer proteins would further form heterotetrameric complexes with other MADS box proteins in the AZ to regulate sepal/petal abscission. It is interesting to note that two MADS box genes, *AGL15* and *AGL18*, have been reported to be expressed in flower organs and in the AZ of flowers<sup>38,39</sup> (Supplementary Fig. 6a–d), and a delay in senescence/abscission of flowers has also been observed in *35S::AGL15* and *35S::AGL18 Arabidopsis* plants<sup>38,39</sup>. The similar delay of flower senescence/abscission (Supplementary Fig. 6e–h) and downregulation of *EDF1-4*, *ERF1*, *BOP1/2*, *IDA*, and *HAESA* (Supplementary Fig. 6i–j) in *35S::AGL15+SRDX Arabidopsis*



supports the notion that AGL15/AGL18 function similarly to FYF/FYL1 as repressors<sup>39</sup> in regulating flower organ abscission. To further explore whether AGL15/AGL18 could also interact with proteins similar to FYF/FYL1 in regulating flower organ abscission, FRET analyses were performed. The results indicated that AGL15/AGL6 are able to form heterodimers with similar efficiency to FYF/AGL6 in the nucleus of tobacco cells (Fig. 2n,

column 6, Fig. 3c). In contrast, AGL18 showed a very weak interaction with AGL6 (Fig. 2n, column 7). This result revealed that AGL15 can form a complex with AGL6, whereas AGL18 might form different protein complexes to perform the redundant function in regulating flower organ abscission.

To test whether FYF (FYL1), AGL6, and AGL15 could form heterotetrameric abscission complexes, a strategy using in vivo

**Fig. 2 Characterization of the *FYL2* gene through transgenic plants and gene expression analysis in *Arabidopsis*.** **a** GUS was stained in the sepals/petals of flowers of *FYL2::GUS Arabidopsis*. GUS staining gradually decreased in the mature flowers during the late stage of flower development. The numbers indicate the different developmental stages of *Arabidopsis* flowers. Bar = 1 mm. Magnified view of stage 7 (**b**), 11 (**c**), and 13 (**d**) *FYL2::GUS* flowers. GUS was strongly and relatively weakly stained in stage 7 young and 11 mature flower buds and was barely detected in stage 13 mature flowers. s: sepal, p: petal, st: stamen. Bars = 0,5 mm. **e** Flowers along the inflorescences of 35S::*FYL2* (first row), 35S::*FYL2*+*SRDX* (second row), 35S::*FYL2*+*VP16* (third row) and wild-type (WT) (fourth row) plants. The numbers indicate the positions of the flowers. Bar = 2 mm. Magnified view of early senescent 35S::*FYL2* (**f**) and 35S::*FYL2*+*VP16* (**h**) flowers and delayed senescent 35S::*FYL2*+*SRDX* (**g**) flowers. s: sepal, p: petal, st: stamen. Bars = 0,5 mm. Detection of *SAG12* (**i**), *EDF1-4* and *ERF1* (**j**) and *BOP1/2*, *IDA* and *HAESA* (**k**) expression in 35S::*FYL2*+*SRDX Arabidopsis*. Error bars show  $\pm$  SD.  $n = 3$  biologically independent samples. The expression of each gene in the transgenic plants is given relative to that of the wild-type plant, which was set at 1. The letter "a", "b" and "c" indicates significant difference from the wild-type (WT) value (a:  $P < 0.05$ , b:  $P < 0.01$ , and c:  $P < 0.001$ ). The two-sided Student's *t*-test was used. **l** Flowers along the inflorescence of 35S::*FYL2*+*SRDX* (top) and wild-type (bottom) plants after exposure to ethylene. Bar = 1 mm. **m** Flowers along the inflorescence of 35S::*FYF*, 35S::*FYF*/35S::*FYL2*, and wild-type (WT) plants. Magnified view of the flower organs that did not become senescent and did not undergo abscission (boxed) in the #7 35S::*FYF* flower. s: sepal, p: petal. Bar = 2 mm. Analysis of the interaction of MADS proteins *FYF*, *FYL1*, *FYL2*, *SOC1*, *AGL19*, *AGL15*, and *AGL18* fused with CFP to *AGL6* (**n**) and *SEP1* (**o**) fused with YFP through the FRET technique. CyPet- and YPet-fused protein pair fluorescence signals were detected in the nucleus expressed in tobacco leaves. CFP and YFP channels were excited with a 440 nm laser, and these two channels were used to calculate the raw FRET signal. FRET values were divided by CFP signals to calculate the FRET efficiency. The average FRET efficiency values were quantified in multiple samples ( $n > 4$ ). Image frame =  $20 \times 20 \mu\text{m}^2$ . N.D. indicates not determined. (Blue line: mean). **p** Analysis of the effect of *FYL2* on *FYF*-*SEP1* interactions. The FRET efficiency for the formation of *FYF*-CFP/*SEP1*-YFP complexes was analyzed in tobacco cells by adding different amounts (0, 25, 75, and 100%) of unlabeled *FYL2* proteins. The average FRET efficiency values were quantified in multiple samples ( $n > 4$ ). Image frame =  $20 \times 20 \mu\text{m}^2$ . (Red line: mean).

FRET based on the distance change and distance symmetry of a stable tetrameric complex in tobacco leaf cells was performed<sup>40</sup>. Since *FYF* is unlikely to interact with *AGL15* (Fig. 3d) in the FRET analysis, we analyzed the possible abscission tetramer containing *FYF*/*AGL6* and *AGL15*/*AGL6* heterodimers. In the *FYF*-*AGL6*-*AGL6*-*AGL15* complex (Fig. 3f–l), the FRET efficiency of the coexpression admixture of *AGL6*:CFP/*FYF*:YFP/*AGL15* (Fig. 3g) was similar to that of *AGL6*:CFP/*AGL15*:YFP/*FYF* (Fig. 3h) (31%/30%) (Fig. 3k), and the distribution range overlapped. The FRET efficiency of the coexpression admixture of *AGL6*:CFP/*AGL6*:YFP/*FYF*/*AGL15* (Fig. 3i) was similar to that of *FYF*:CFP/*AGL15*:YFP/*AGL6*/*AGL6* (Fig. 3j) (29%/24%) (Fig. 3k), and the distribution range overlapped.

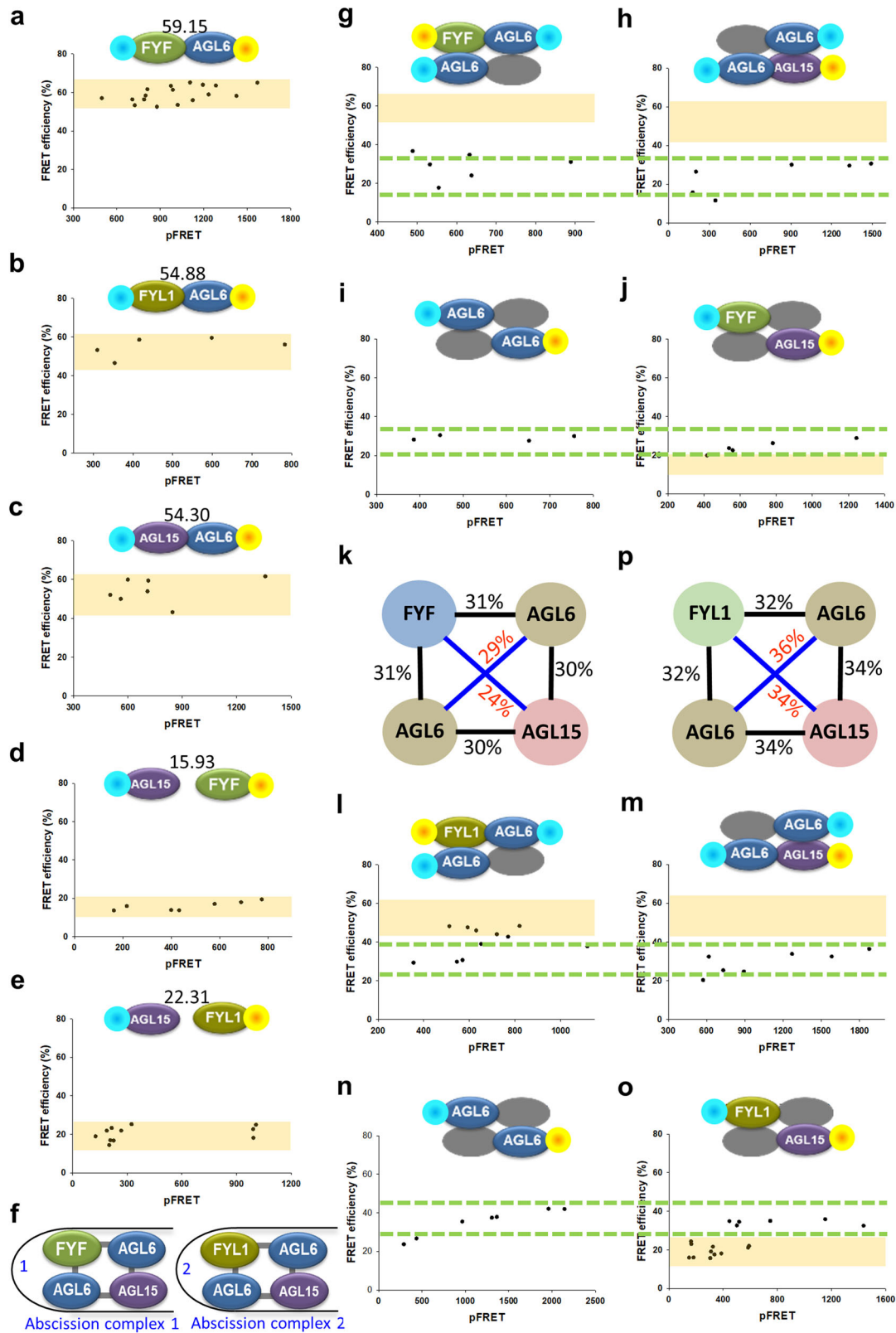
Similarly, *FYL1* was unlikely to interact with *AGL15* (Fig. 3e), and the FRET efficiency of the coexpression admixture of *AGL6*:CFP/*FYL1*:YFP/*AGL15* (Fig. 3l) was similar to that of *AGL6*:CFP/*AGL15*:YFP/*FYL1* (Fig. 3m) (32%/34%) (Fig. 3p), and the distribution range overlapped. Similarly, the FRET efficiency of the coexpression admixture of *AGL6*:CFP/*AGL6*:YFP/*FYL1*/*AGL15* (Fig. 3n) was similar to that of *AGL15*:CFP/*FYL1*:YFP/*AGL6*/*AGL6* (Fig. 3o) (36%/34%) (Fig. 3p), and the distribution range overlapped. These overlapped patterns for the distribution range observed for *FYF*-*AGL6*-*AGL6*-*AGL15* and *FYL1*-*AGL6*-*AGL6*-*AGL15* heterotetrameric complexes were similar to that for the most stable heterotetrameric complexes *PI-AP3-AG-SEP3* described in our previous study<sup>40</sup>. These results indicated that *FYF*-*AGL6*-*AGL6*-*AGL15* and *FYL1*-*AGL6*-*AGL6*-*AGL15* are likely stable heterotetrameric complexes in regulating flower organ abscission. In addition, *FYF*-*AGL6*-*AGL6*-*AGL15* is also likely a stable heterotetrameric complex in regulating flower organ senescence.

***FYL2* can interact with *AGL6* and *SEP1* in regulating flower senescence.** Similarly, the investigation of whether *FYL2* could also interact with proteins similar to *FYF* in regulating flower organ senescence was also performed using FRET analyses. When *FYL2*-CFP and *AGL6*-YFP or *SEP1*-YFP were used to observe the physical interactions of *FYL2* and *AGL6* or *SEP1*, a lower efficiency of *FYL2*/*AGL6* heterodimer formation than that of *FYF*/*AGL6* (Fig. 2n, column 1) in the nucleus of tobacco cells was observed (Fig. 2n, column 3). The efficiency for the formation of *FYL2*/*SEP1* (Fig. 2o, column 3) was also lower than that for *FYF*/*SEP1* (Fig. 2o, column 1). These results suggested that similar to

*FYF*, *FYL2* can also interact with *AGL6* and *SEP1* to form senescence complexes, although at a lower efficiency. Since *FYL2* was only expressed in the flower organs of sepals/petals, which overlapped with part of *AGL6* and *SEP1* expression, these data revealed that *FYL2* can physically interact with *AGL6* and *SEP1* during *Arabidopsis* flower development to regulate sepal/petal senescence.

Since we have already shown that *FYL2* functions opposite to *FYF* in controlling sepal/petal senescence, *FYL2* might compete to bind the interacting protein to form a functional complex. To examine this assumption, FRET efficiency for the formation of *FYF*-CFP/*SEP1*-YFP complexes was examined in tobacco cells by adding different amounts of unlabeled *FYL2* proteins. The results indicated that the efficiency for *FYF*-CFP to interact with *SEP1*-YFP (Fig. 2p, column 1) was clearly decreased by the presence of 25–75% of the *FYL2* proteins (Fig. 2p, columns 2 and 3). The ability of *FYF*-CFP to interact with *SEP1*-YFP was almost completely competed for by the presence of 100% *FYL2* protein (Fig. 2p, column 4). Thus, *FYL2* competes with *FYF* to interact with *SEP1*, performing opposite functions in controlling sepal/petal senescence.

***FYF*-like genes *AGL19/14* and *SOC1* are complementary to *FYF* in regulating flower senescence.** We found a possible mechanism involving three *FYF*-like genes (*FYF* and *FYL1/2*) in regulating flower organ senescence and abscission. It is interesting to note that three other genes in the *SOC1* subgroup, *AGL19*, *AGL14* (*XAL2*), and *AGL20* (*SOC1*), were also closely related to the *FYF*/*FYL1*/*FYL2* genes (Supplementary Figs. 1, 2)<sup>6,16</sup>. Do these three genes also harbor similar functions to *FYF*/*FYL1*/*FYL2* in regulating flower senescence/abscission? Interestingly, similar to that observed in 35S::*FYF* and 35S::*FYF*+*SRDX Arabidopsis*, a strong delay in flower senescence and abscission (Fig. 4a–c), insensitivity to ethylene treatment (Fig. 4d–i) and downregulation of *EDF1-4*, *ERF1*, *BOP2*, *IDA*, and *HAESA* (Fig. 4j, k) were observed in 35S::*AGL19* and 35S::*AGL19*+*SRDX Arabidopsis*. In contrast to *AGL19*, only 35S::*AGL14*+*SRDX* and 35S::*SOC1*+*SRDX* caused a strong delay in flower senescence/abscission and a downregulation of senescence/abscission-related genes (Supplementary Figs. 7a–d, 8a–c), whereas no or a reduced effect was seen in 35S::*AGL14* and 35S::*SOC1* plants. These results indicated that *AGL19* and *AGL14*/*SOC1* functioned as strong and weak repressors, respectively, and that part of their function



complemented *FYF* in suppressing flower organ senescence/abscission.

Similar to the expression pattern of *FYF/FYL2*, higher *AGL19/AGL14/SOC1* expression was observed during early flower development (before stage 9) than during late developmental stages (after stage 12) (Fig. 4l and Supplementary Figs. 7e, 8d), which further revealed possible similar and overlapping functions

of *FYF* and *AGL19/AGL14/SOC1*. GUS staining was detected in sepal/petal organs and was absent in the AZ of *AGL19::GUS* (Fig. 4m, n) and *SOC1::GUS* flowers (Supplementary Fig. 8e-g), suggesting that *AGL19/14* and *SOC1* might have part of the functions of *FYF* in regulating flower senescence but not abscission. Although *SOC1* and *AGL19* might also be involved in regulating flower senescence, they have very low or complete

**Fig. 3 The distance-measuring system validated that *Arabidopsis* AGL15-AGL6 forms stable abscission tetrameric complexes with FYF-AGL6 and FYL1-AGL6.** The steady state of dimerization of the protein complexes FYF-AGL6 (a), FYL1-AGL6 (b), AGL15-AGL6 (c), FYF-AGL15 (d), and FYL1-AGL15 (e) is revealed in scatter diagrams showing pFRET and FRET efficiency. The black dots show the independent cell nuclei, and the yellow boxes indicate the steady-state FRET efficiency range for the protein complex. The mean value of FRET efficiency in the steady state is shown at the top of the schematic model, which is the baseline. The protein fused with CFP/YFP was attached by blue/yellow spots. f Schematic model of the protein interactions in the *Arabidopsis* abscission complexes (1) FYF-AGL6-AGL6-AGL15 and (2) FYL1-AGL6-AGL6-AGL15. Scatter diagram of the raw FRET (pFRET) and FRET efficiency values of the dimer pairs in adjacent lines AGL6-FYF (g) and AGL6-AGL15 (h) and diagonal lines AGL6-AGL6 (i) and FYF-AGL15 (j) in the abscission complex FYF-AGL6-AGL6-AGL15, with a different number of cell nuclei measured. The green dotted lines indicate the overlapping distribution range at the steady state. The yellow boxes (in g, h, j) indicate the baselines obtained for the dimer pairs. The protein fused with CFP/YFP was attached by blue/yellow spots. k Schematic model and FRET efficiency of four different pairs (two adjacent lines and two diagonal lines) of the protein interactions in the *Arabidopsis* stable abscission complex FYF-AGL6-AGL6-AGL15. The two adjacent lines (black) show similar FRET efficiencies (31%/30%), and the two diagonal lines (blue) show similar FRET efficiencies (29%/24%). Scatter diagram of the raw FRET (pFRET) and FRET efficiency values of the dimer pairs in adjacent lines AGL6-FYL1 (l) and AGL6-AGL15 (m) and diagonal lines AGL6-AGL6 (n) and FYL1-AGL15 (o) in the abscission complex FYL1-AGL6-AGL6-AGL15, with a different number of cell nuclei measured. The green dotted lines indicate the overlapping distribution range at the steady state. The yellow boxes (in l, m, o) indicate the baselines obtained for the dimer pairs. The protein fused with CFP/YFP was attached by blue/yellow spots. p Schematic model and FRET efficiency of four different pairs (two adjacent lines and two diagonal lines) of the protein interactions in the *Arabidopsis* stable abscission complex FYL1-AGL6-AGL6-AGL15. The two adjacent lines (black) show similar FRET efficiencies (32%/32%), and the two diagonal lines (blue) show similar FRET efficiencies (36%/34%).

no interactions with AGL6 (Fig. 2n, columns 4, 5) or SEP1 (Fig. 2o, columns 4, 5). This result indicated that the *FYF*/*FYL1*/*FYL2* and *AGL19/14/SOC1* groups might have evolved to have their own interacting partners in regulating flower senescence/abscission.

***FYF* activates *FYL1* and *AGL19/14/SOC1* expression to enhance the regulation of flower abscission and senescence.** Since *FYF* has the same function as *FYL1* and *AGL19/14/SOC1* to regulate abscission and senescence of the sepal/petal, respectively, we were also interested in determining how they work together. When the expression pattern of endogenous *FYL1* and *AGL19/14/SOC1* was analyzed in 35S::*FYF* flowers, we found that the expression of all three genes was clearly upregulated (Fig. 4o). Our results revealed that *FYL1* was activated by *FYF* in the AZ during flower development and could enhance the function of the *FYF* gene in suppressing sepal/petal abscission, whereas *AGL19/14/SOC1* were activated by *FYF* in sepals/petals during flower development, which could enhance the function of the *FYF* gene in suppressing sepal/petal senescence. Interestingly, we found that *FYF*, *FYL1*, *AGL14*, and *SOC1* expression was also upregulated in 35S::*AGL19* flowers (Fig. 4p). This result suggested that *FYF* and other *FYF*-like genes with the strong repressor role, such as *AGL19*, could reciprocally activate each other to enhance the suppression of sepal/petal senescence.

***FYF* activates *FYL2* expression to regulate flower senescence possibly through a feedback loop.** Exploring how *FYF* competes with *FYL2* to oppositely regulate sepal/petal senescence is interesting. When the expression pattern of endogenous *FYL2* was analyzed in 35S::*FYF* flowers, we found that *FYL2* expression was upregulated (Fig. 4o). Our results revealed that *FYL2* was activated by *FYF* during flower development and that *FYL2* could possibly form a feedback loop to contend with endogenous *FYF* function and to more appropriately control flower senescence. This assumption was further supported by the downregulation of *FYL2* expression in *fyf/agl15* double mutants (Supplementary Fig. 9a). We also found that *FYL2* expression was upregulated in 35S::*AGL19* flowers (Fig. 4p). This result suggested that *FYF* and *AGL19* might control sepal/petal senescence by regulating *FYL2* in a similar way.

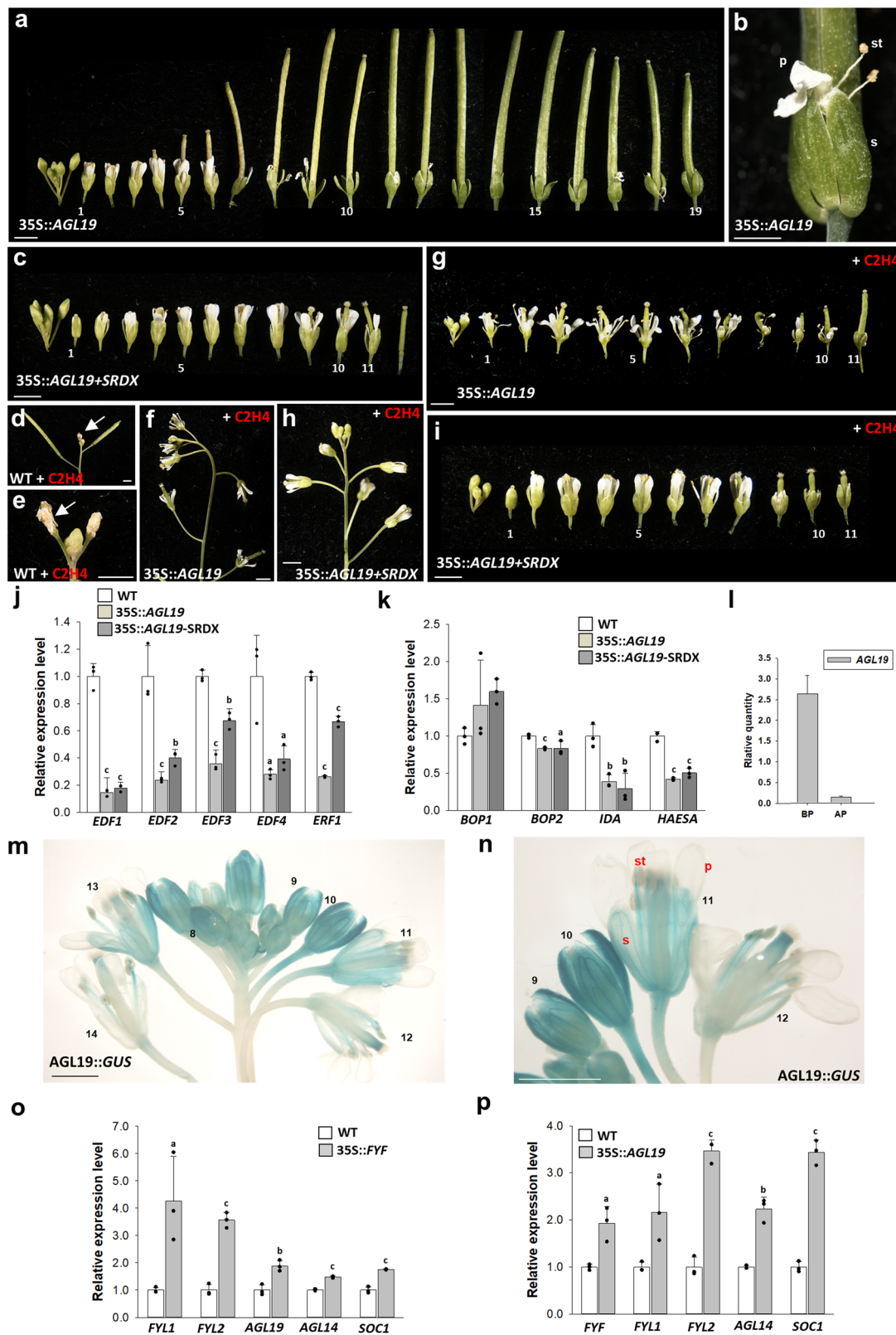
## Discussion

The *Arabidopsis* MADS box gene *FYF* can regulate flower organ senescence and abscission<sup>1</sup>. Ectopic expression of *FYF* caused a delay of senescence and a deficiency of abscission in flowers of transgenic *Arabidopsis* and *Eustoma grandiflorum*<sup>1</sup>. This study further showed that two tandem repeat *FYF*-like genes, *FYL1*, and *FYL2*, and three other *FYF*-like genes, *AGL19/14* and *SOC1*, in *Arabidopsis* were also involved in the regulation of flower organ abscission and/or senescence, and their functions were complementary or antagonistic to *FYF*.

*FYL1* was found to act as a repressor to suppress abscission in sepals/petals with a complementary function to *FYF* (Fig. 5a). Unexpectedly, *FYL2* could function as an activator and antagonize *FYF* in promoting the senescence of sepals/petals (Fig. 5a). The functions of *FYL1/2* are correlated with their expression pattern since *FYL1* was specifically expressed in the AZ of sepals/petals, whereas *FYL2* expression was detected in the organs of sepals/petals. The amino acid identity and the phylogenetic tree relationship<sup>6</sup> revealed that *FYL1/2* were possibly the result of two duplication events. The first event generated an *FYL1/2* ancestor from *FYF*, and the second event produced the two tandem repeats *FYL1* and *FYL2* from this *FYL1/2* ancestor. The conserved role of *FYF*/*FYL1*/*FYL2* during evolution in regulating flower senescence and/or abscission was further supported by their ability to interact with the same MADS box proteins AGL6 and SEP1. The original *FYF* gene must have contained both regulatory elements in its promoter or introns<sup>1,33,41–45</sup>, which are required for its expression in the organs and AZ of sepals/petals. In the AZ, *FYF* specifically interacts with AGL6 to suppress abscission of the sepals/petals (Fig. 5a, b). In the sepal/petal organs, *FYF* can interact with either AGL6 or SEP1 to suppress senescence (Fig. 5a, c). In the tandem repeat genes *FYL1* and *FYL2*, the subfunctional alteration of the regulatory elements during evolution resulted in restriction of the expression of *FYL1* in the AZ and *FYL2* in sepal/petal organs. *FYL1* should maintain the conserved ability of *FYF* to interact with AGL6 together to suppress the abscission of sepals/petals (Fig. 5a, b). Conversely, *FYL2* only retained the conserved ability of *FYF* to interact with AGL6 and SEP1 in regulating sepal/petal senescence (Fig. 5a, c). However, *FYL2* evolved into a role antagonistic to *FYF* and possibly helped to control *FYF* activity through a feedback loop to protect the flower buds from senescence and ensure the final senescence of the mature flowers (Fig. 5a, c).

In addition to *FYL1/2*, three putative *FYF*-like genes in the *SOC1* subgroup, *AGL19*, *AGL14*, and *SOC1*, which are closely





related to *FYF/FYL1/FYL2* genes based on the phylogenetic tree relationship<sup>6,16</sup>, were also characterized. Based on the results of the functional analysis and the expression patterns of these three genes, we found that *AGL19*, *AGL14*, and *SOC1* were all involved in the regulation of senescence but not abscission of flower organs (Fig. 5a, c). *AGL19* might play a stronger repressive role than *AGL14/SOC1*, which functions similarly to *FYF* in suppressing

flower senescence (Fig. 5a). Although *AGL19/14* and *SOC1* were found to be involved in regulating flower senescence, similar to *FYF/FYL2*, they seemed to perform their function in a different way in terms of finding interacting partners to form functional complexes. For example, *FYF/FYL1/FYL2* can interact sufficiently with *AGL6/SEP1*, whereas *AGL19/14/SOC1* can not interact with *AGL6/SEP1*. This finding indicated that the *AGL19/14/*

**Fig. 4 Characterization of the AGL19 gene through transgenic plants and gene expression analysis in Arabidopsis.** **a** Flowers along the inflorescence of 35S::AGL19 plants. The numbers indicate the positions of the flowers. Bars = 2 mm. **b** Magnified view of the flower organs of a 35S::AGL19 flower that were not senescent/abscised from (**a**). s: sepal, p: petal, st: stamen. Bars = 0.5 mm. **c** Flowers along the inflorescence of 35S::AGL19+SRDX plants. The numbers indicate the positions of the flowers. Bars = 2 mm. Flowers along the inflorescence of wild-type (**d, e**), 35S::AGL19 (**f, g**), and 35S::AGL19+SRDX (**h, i**) plants after exposure to ethylene. Wild-type flowers were senescent (arrowed in **d, e**), whereas 35S::AGL19 and 35S::AGL19+SRDX flowers were not senescent/abscised. Bars = 2 mm. Detection of *EDF1-4* and *ERF1* (**j**) and *BOPI/2*, *IDA* and *HAESA* (**k**) expression in 35S::AGL19 and 35S::AGL19+SRDX *Arabidopsis*. Error bars show  $\pm$  SD.  $n = 3$  biologically independent samples. The expression of each gene in the transgenic plants is given relative to that of the wild-type plant, which was set at 1. The letter "a", "b" and "c" indicates significant difference from the wild-type (WT) value (a:  $P < 0.05$ , b:  $P < 0.01$ , and c:  $P < 0.001$ ). The two-sided Student's *t*-test was used. **l** Detection of *AGL19* expression before (BP) and after (AF) pollination. **m, n** GUS was stained in the sepals/petals of flowers of AGL19::GUS *Arabidopsis*. GUS was strongly stained in stage 8–10 young flower buds and gradually decreased in the mature flowers during the late stage (after stage 12) of flower development. The numbers indicate the different developmental stages of *Arabidopsis* flowers. **n** is the magnified view from (**m**). s: sepal, p: petal, st: stamen. Bars = 1 mm. Detection of *FYL1/FYL2/AGL19/AGL14/SOC1* expression in 35S::FYF *Arabidopsis* (**o**) and *FYF/FYL1/FYL2/AGL14/SOC1* expression in 35S::AGL19 *Arabidopsis* (**p**). Error bars show  $\pm$  SD.  $n = 3$  biologically independent samples. The expression of each gene in the transgenic plants is given relative to that of the wild-type plant, which was set at 1. The letter "a", "b" and "c" indicates significant difference from the wild-type (WT) value (a:  $P < 0.05$ , b:  $P < 0.01$ , and c:  $P < 0.001$ ). The two-sided Student's *t*-test was used.

SOC1 subgroup might have their own interacting partners in regulating flower senescence that differ from those of FYF/FYL1/FYL2 during evolution.

One interesting finding is that these FYF-like genes could regulate the expression of each other. For example, FYF could positively regulate the expression of FYL1 and AGL19/14/SOC1 to enhance suppression of the abscission and senescence of flower organs, respectively, whereas AGL19 could positively regulate the expression of FYF and AGL14/SOC1 to enhance the suppression of flower organ senescence. This positive reciprocal regulatory network among the FYF-like genes should provide a mechanism to ensure the suppression of senescence/abscission during the early stage of flower organ development (Fig. 5b, c). In addition, we also found a possible feedback loop regulatory mechanism between FYF and its opposite functional activator FYL2. FYF could activate the expression of FYL2, which possibly sequentially antagonized the activity of FYF. In this case, FYF activity will be countervailed at an appropriate level by FYL2, which is high in early and low in late flower development and ensures that sepal/petal senescence will occur after flower maturation and will not occur in the flower bud stage (Fig. 5c).

In addition to the FYF-like genes studied, we also found that one other MADS box protein, AGL15, which has also been characterized to be able to regulate flower organ senescence/abscission (Fig. 5a)<sup>38,39</sup>, was able to interact with AGL6 to form stable heterotetrameric abscission complexes (FYF-AGL6-AGL6-AGL15 and FYL1-AGL6-AGL6-AGL15) and a senescence complex (FYF-AGL6-AGL6-AGL15) with FYF/FYL1 (Fig. 5b, c). Interestingly, AGL18, a closely related gene to AGL15<sup>38,39</sup>, has no interaction with AGL6 to form further heterotetrameric abscission/senescence complexes with FYF/FYL1. Thus, despite redundant functions, AGL15 and AGL18 may interact with their specific partners to form different protein complexes to regulate flower organ abscission/senescence (Fig. 5d).

A scenario was proposed to elucidate the evolutionary modification of the functions and complicated network of FYF-like genes in regulating flower senescence/abscission. In *Arabidopsis*, an FYF-like ancestor duplicated into two subgroups of genes (FYF/FYL1/FYL2 and AGL19/AGL14/SOC1) and eventually evolved to divergent functions through subfunctionalization in regulating various flower development processes, including senescence/abscission. In the FYF subgroup, FYF has both functions in suppressing flower senescence and abscission, whereas FYL1 only suppresses flower abscission, and FYL2's function is converted into the activation of flower senescence (Fig. 5a). In the SOC1 subgroup, AGL19, AGL14, and SOC1 showed only one function in suppressing flower senescence, with the effect of AGL19 being stronger than that of AGL14/SOC1 (Fig. 5a). FYF-

like proteins can form heterotetrameric complexes with A/E functional proteins (AGL6, SEP1, and unidentified X) and AGL15/18-like proteins (AGL15/18 and unidentified Y) to perform their functions (Supplementary Fig. 2 and Fig. 5d). In the AZ, FYF/AGL6/AGL6/AGL15 and FYL1/AGL6/AGL6/AGL15 were two identified heterotetrameric abscission complexes that suppressed flower abscission (Fig. 5b). In sepals/petals, we identified FYF/AGL6/AGL6/AGL15 together with FYF/SEP1/Y, AGL19/X/Y, AGL14/X/Y, and SOC1/X/Y heterotetrameric senescence complexes in suppressing flower senescence (Fig. 5c).

Our findings reveal the potential immense complexity of the different combinations of FYF-like, A/E functional, and AGL15/18-like proteins in forming heterotetrameric abscission/senescence complexes (Fig. 5d). This complicated gene redundancy might explain why it is difficult to identify the senescence/abscission mutant phenotype in a single gene mutation for these genes. In an attempt to mutate FYF (key gene in FYF-like) and AGL15 (key gene in AGL15/18-like) simultaneously, T-DNA mutants for each gene were crossed to generate *fyf/agl15* double mutations. Very interestingly, early senescence and abscission of the flowers was observed in these *fyf/agl15* double mutants (Supplementary Fig. 9). This result strongly supported our assumption that abscission/senescence heterotetrameric complexes are at least composed of different combinations of FYF-like and AGL15/18-like proteins. Simultaneous mutations in FYF and AGL15 proteins will disrupt the functions of various combinations of the complexes and result in early senescence/abscission mutant phenotypes. In conclusion, our findings not only greatly expand the current knowledge concerning the multifunctional evolution of FYF-like genes in regulating flower senescence/abscission but also provide an excellent example for the study of diverse functionalizations of duplicate gene pairs in plants.

## Methods

**Plant materials and growth conditions.** The T-DNA insertion mutants of FYF (*fyf*, SALK\_047915) and AGL15 (*agl15*, SALK\_076234C) mutants *Arabidopsis* seeds were obtained from the Arabidopsis Biological Resource Center, Ohio State University, Columbus, OH, USA. Seeds for *Arabidopsis* were germinated and grown as described previously<sup>1,2,46</sup>. *Arabidopsis* seeds were sterilized and placed on agar plates containing 1/2 X Murashige & Skoog medium<sup>47</sup> at 4 °C for 2 days. Before being transplanted to soil, the seedlings were grown in growth chambers under long-day conditions (16 h light/8 h dark) at 22 °C for 10 days. The light intensity of the growth chambers was 150  $\mu\text{E m}^{-2} \text{s}^{-1}$ .

**Cloning of the cDNA for FYL1, FYL2, AGL6, AGL19, AGL14, SOC1, and AGL15 from Arabidopsis.** For 35S::MADS constructs, the cDNAs for FYL1, FYL2, AGL6, AGL19, AGL14, SOC1, and AGL15 were obtained by PCR amplification using gene-specific 5' and 3' primers. The primers contained the *Xba*I and *Kpn*I recognition sites to facilitate the cloning of the cDNAs. The *Xba*I-*Kpn*I fragment containing the cDNA was cloned into the binary vector pEYon-22K<sup>1</sup> under the control of the

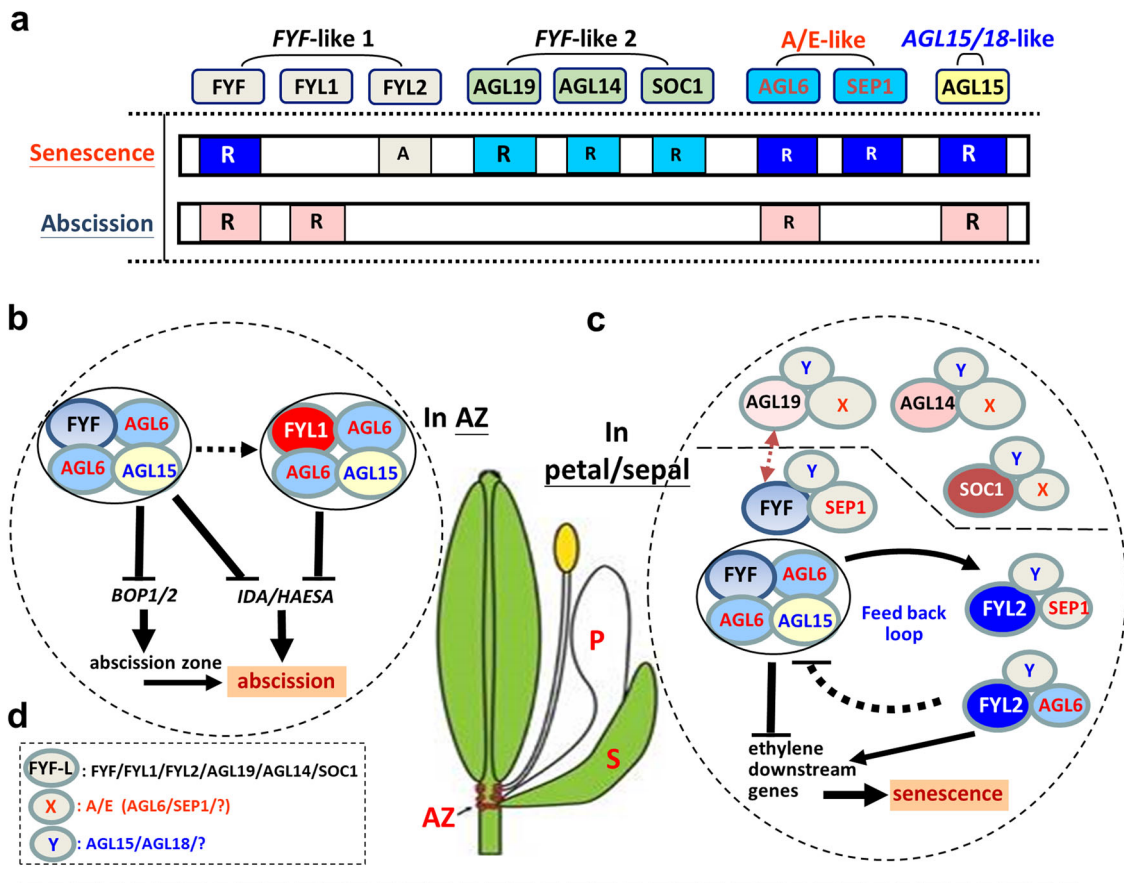


**Fig. 5** The functional evolution and regulatory network of the FYF-like genes in regulating flower senescence/abscission. **a** In *Arabidopsis*, six FYF-like genes in two subgroups (FYF/FYL1/FYL2 and AGL19/AGL14/SOC1) were all involved in regulating flower senescence and/or abscission. In the FYF subgroup, FYF acts as a repressor (R) in suppressing both flower senescence (indicated by a blue box) and abscission (indicated by a pink box), and FYL1 acts as a repressor (R) and only suppresses flower abscission (indicated by a pink box). FYL2 functions as an activator (A) in promoting flower senescence (indicated by a gray box). In the SOC1 subgroup, AGL19, AGL14, and SOC1 function as repressors (R) and have only one function in suppressing flower senescence (indicated by a light blue box), with the effect of AGL19 being stronger than that of AGL14/SOC1. In addition, the A/E functional genes AGL6/SEP1 and AGL15/18-like gene AGL15 (as a repressor) can regulate senescence (indicated by a blue box) by interacting with FYF/FYL2, whereas AGL6 and AGL15 can also regulate abscission (indicated by a pink box) by interacting with FYF/FYL1. The size of the letter R in the box correlated with the strength of the repressor for the MADS box proteins. **b** In the AZ of the perianth, FYF and FYL1 complement each other by forming two identified heterotetrameric abscission complexes, FYF/AGL6/AGL6/AGL15 and FYL1/AGL6/AGL6/AGL15, suppressing flower abscission through the downregulation (–) of BOP1/2 and IDA/HAESA expression. **c** In sepals/petals, FYF, AGL19, AGL14, and SOC1 functioned antagonistically to FYL2 in suppressing flower senescence. An identified FYF/AGL6/AGL6/AGL15 together with FYF/SEP1/Y, AGL19/X/Y, AGL14/X/Y, and SOC1/X/Y heterotetrameric senescence complexes suppressed sepal/petal senescence through the downregulation (–) of ethylene downstream gene expression. In contrast, FYL2/AGL6/Y and FYL2/SEP1/Y heterotetrameric complexes promoted sepal/petal senescence by the activation (→) of ethylene downstream gene expression, possibly through a negative feedback loop to FYF/X/Y, AGL19/X/Y, AGL14/X/Y, and SOC1/X/Y. **d** In these cases from (c), the heterotetrameric complexes are composed of FYF-like, X (in red) and Y (in blue) proteins. FYF-like can be either one of the FYF/FYL1/FYL2/AGL19/AGL14/SOC1, X can be AGL6, SEP1, or any unidentified A/E proteins, whereas Y can be AGL15, AGL18, or any unidentified AGL15/18-like proteins.

CaMV 35S promoter and used for plant transformation. Sequences for the primers are listed in the Supplementary Table 1.

**Cloning of the promoter DNA fragment from *Arabidopsis*.** For the FYL1::GUS and FYL2::GUS constructs, the promoter regions which included the 5'UTR and first intron for FYL1 (2.65 kb) and FYL2 (2.43 kb) were obtained by PCR amplification using specific primer pairs from the genomic DNA followed by cloning into the pGEM-T easy vector (Promega, Madison, WI, USA). These promoter fragments were then subcloned into the linker region before the  $\beta$ -Glucuronidase (GUS) coding region in the binary vector pEpyon01k<sup>1,2</sup>. For the AGL6::GUS, AGL15::GUS, AGL19::GUS, and SOC1::GUS constructs, the promoter regions which included the 5'UTR and first intron for AGL6 (4.96 kb), AGL15 (0.94 kb), AGL19 (4.59 kb) and SOC1 (5.68 kb) were obtained by PCR amplification and these promoter fragments were subcloned into the linker region before the  $\beta$ -Glucuronidase (GUS) coding region in the binary vector pEpyon01k in the same manner as FYL1/2::GUS. Sequences for the primers are listed in Supplementary Table 1. For the IDA::FYL1 construct, the IDA promoter (1.43 kb) was obtained by PCR amplification as described previously<sup>1</sup>. The cDNA for FYL1 was obtained by

PCR amplification. The IDA promoter and the cDNA for FYL1 were subcloned into the modified binary vector pEpyon-12K<sup>1</sup>. Sequences for the primers are listed in Supplementary Table 1.

**Construction of the MADS + SRDX constructs.** For the 35S::FYL1+SRDX, 35S::FYL2+SRDX, 35S::AGL6+SRDX, 35S::AGL15+SRDX, 35S::AGL19+SRDX, 35S::AGL14+SRDX, 35S::SOC1+SRDX constructs, the cDNAs for FYL1/FYL2/AGL6/AGL15/AGL19/AGL14/SOC1 were obtained by PCR amplification and cloned into the pEpyon-2aK plasmid upstream of the SRDX (LDLDELRLGFA\*) sequence, under the control of the CaMV 35S promoter as described previously<sup>1,2</sup>. The sequences for the primers are listed in Supplementary Table 1.

**Construction of the MADS + VP16 constructs.** For the 35S::FYL1+VP16, and 35S::FYL2+VP16 construct, the cDNAs for FYL1/FYL2 were obtained by PCR amplification and cloned into the pEpyon-2bK plasmid upstream of the VP16-AD fragment sequence, under the control of the CaMV 35S promoter as described previously<sup>1,2</sup>. The sequences for the primers were listed in Supplementary Table 1.

**Plant transformation and transgenic plant analysis.** A floral dip method as described elsewhere<sup>48</sup> was used to introduce constructs made in this study in the *Agrobacterium tumefaciens* strain GV3101 into *Arabidopsis* plants. PCR and RT-PCR analyses were used to verify the transformants that survived in medium containing kanamycin (50 µg/ml). To generate 35S::FYF/35S::FYL2 *Arabidopsis*, constructs of 35S::FYL2 which contained hygromycin resistant gene were co-transformed with 35S::FYF (kanamycin resistant) into *Arabidopsis* plants. Transformants that survived in medium containing both kanamycin (50 µg/ml) and hygromycin (5 µg/ml) were selected for further analysis. To generate *fyf/agl15* double mutant *Arabidopsis*, homozygous *fyf* were crossed with the *agl15* T-DNA mutants in the Columbia background and F<sub>1</sub> plants were used to further generate the F<sub>2</sub> generation. One quarter of the F<sub>2</sub> plants were *fyf/agl15* and were further verified and selected for further analysis.

**Histochemical GUS assay.** Histochemical staining was performed under standard method described previously<sup>2,49,50</sup>. Samples were incubated in solution (0.05 mM Potassium ferricyanide, 0.05 mM Potassium ferrocyanide, 100 mM Phosphate buffer, pH 7.0) containing 2 mM X-Gluc (5-bromo-4-chloro-3-indolyl β-D-glucuronic acid) for several hours at 37 °C. The sample was examined under a dissecting microscope.

**Real-time PCR analysis.** For real-time quantitative RT-PCR, the reaction was performed on a MJ Opticon system (MJ Research, Waltham, MA) using SYBR<sup>®</sup> Green Real-time PCR Master Mix (TOYOBO Co., LTD.). The amplification condition was 95 °C for 10 min, followed by 40 cycles of amplification (95 °C for 15 s, 58 °C for 15 s, 72 °C for 30 s and then plate reading) and melted (50–95 °C with plate readings every 1 °C) as described previously<sup>1,2</sup>. Sequences for the primers used for real-time quantitative RT-PCR for *FYF*, *FYL1*, *FYL2*, *AGL6*, *AGL15*, *AGL19*, *AGL14*, *SOCI1*, *EDF1*, *EDF2*, *EDF3*, *EDF4*, *ERF1*, *SAG12*, *BOPI1*, *BOP2*, *IDA*, and *HAESA*, were listed in Supplementary Table 1. The housekeeping gene *UBQ10* was used as normalization control with the following primers: RT-UBQ10-1 and RT-UBQ10-2<sup>51</sup>. Data were analyzed using Gene Expression Macro software (version 1.1, Bio-Rad).

**Ethylene responses.** As described previously<sup>1,52</sup>, wild-type and transgenic *Arabidopsis* plants were sealed in plastic chambers and gassed with air or air containing 10 ppm ethylene for 3 days in a 16 h light/8 h dark cycle and phenotype analyzed.

**FRET analysis.** The procedure used to prepare FRET-associated fusion constructs was described in previous studies<sup>36,53</sup>. To fuse FYF/FYL1/FYL2/AGL6/SEPI/AGL15/AGL18/AGL19/SOCI1 with CFP or YFP, the cDNAs for *Arabidopsis* *FYF*/*FYL1*/*FYL2*/*AGL6*/*SEPI*/*AGL15*/*AGL18*/*AGL19*/*SOCI1* were obtained by PCR amplification using gene-specific primers and cloned into the pEpyon-36K and pEpyon-37K vectors upstream of the CFP or YFP sequence under the control of the CaMV 35S promoter. The following gene-specific primers were used: *FYF*, *FYF-FRET-F-PstI* (5'-CTGCAGATGGTTAGAGGAAAGATAGAGATGAAG-3') and *FYF-FRET-R-ns-SalI* (5'-GTCGACGCAGTTTCTATTGGCAAACCG-3'); *FYL1*, *FYL1-FRET-F-XbaI* (5'-TCTAGAATGGTGTAGAGGGAAGATCGAGATC-3') and *FYL1-FRET-R-ns-kpnI* (5'-GGTACCTAGCCGAGTCCAGGGCAATC-3'); *FYL2*, *FYL2-FRET-F-XbaI* (5'-TCTAGACTGCAGATGGGAAGGGGAAGAGTTGA-3') and *FYL2-FRET-R-ns-kpnI* (5'-GGTACCTGGTCCGTTCTTCAGAAATCC-3'); *AGL6*, *AGL6-FRET-F-XbaI* (5'-TCTAGAATGGGAAGGGGAGAGTTGG-3') and *AGL6-FRET-R-ns-kpnI* (5'-GGTACCAAGAACCCCAACCTTGGAGC-3'); *SEPI*, *SEPI-FRET-F-pstI* (5'-CTGCAGATGGGAAGAGGAAGAGTAGAGCTGAA-GAG-3') and *SEPI-FRET-R-ns-SalI* (5'-GTCGACGAGCATCCACCCCGG-GATGT-3'); *AGL15*, *AtAGL15-FRET-F-XbaI* (5'-TCTAGAATGGGTGGTGGAAAATCGAG-3') and *AtAGL15-FRET-R-ns-kpnI* (5'-GGTACCAACAGAGA-GAACCTTTGTCTTTGGC-3'); *AGL18*, *AtAGL18-FRET-F-XbaI* (5'-TCTAGAATGGGTGGGGAAGATAGA-3') and *AtAGL18-FRET-R-ns-kpnI* (5'-GGA-TCCATCAGAAGCCACTTGACTCC-3'); *AGL19*, *AtAGL19-FRET-F-XbaI* (5'-TCTAGAATGGTGGGGAAGGCAAAACG-3') and *AtAGL19-FRET-R-ns-kpnI* (5'-GGTACCAATTTTGGAGGGAATTTTGGATTGTC-3'); *SOCI1*, *AtSOCI1-FRET-F-XbaI* (5'-TCTAGAATGGTGGGGAAGGCAAAACTC-3') and *AtSOCI1-FRET-R-ns-kpnI* (5'-GGTACCCTTTCTTGAAGAACAAGGTAACCAATG-3'). These constructs were transformed into the *Agrobacterium* strain C58C1. Different ectopic proteins were expressed in tobacco cells and a confocal microscope was used to detect the fluorescence signals in the nucleus. To perform the subcellular localization assay, *Agrobacterium*-infiltrated *N. benthamiana* leaves were vacuum infiltrated in 10 mM MgCl<sub>2</sub> at room temperature until immersed. As previously described<sup>36,52</sup>, an Olympus FV1000 confocal microscope (Olympus FV1000, Tokyo, Japan) and the FV-ASW 3.0 software were used to visualize fluorophores and to calculate the raw FRET and FRET efficiency values. To evaluate the variation in protein interaction distances among different protein complexes ( $n > 4$ ), the mean value of FRET efficiency in the nucleus was calculated.

**Statistics and reproducibility.** Data in the analysis of gene expression in various transgenic plants were analyzed using the two-sided Student's *t*-test and represented as the mean ± SD. In these cases,  $n = 3$  biologically independent samples.

The letter “a”, “b” and “c” indicates significant difference from the wild-type (WT) value (a:  $P < 0.05$ , b:  $P < 0.01$ , and c:  $P < 0.001$ ).

**Reporting summary.** Further information on research design is available in the Nature Research Reporting Summary linked to this article.

## Data availability

The data supporting the findings of this work are available within the paper and the Supplementary Information files. The data sets generated and analyzed during this study are available from the corresponding author upon request.

Received: 11 January 2022; Accepted: 24 June 2022;

Published online: 05 July 2022

## References

- Chen, M. K. et al. The MADS box gene, *FOREVER YOUNG FLOWER*, acts as a repressor controlling floral organ senescence and abscission in *Arabidopsis*. *Plant J.* **68**, 168–185 (2011).
- Chen, W. H., Li, P. F., Chen, M. K., Lee, Y. I. & Yang, C. H. *FOREVER YOUNG FLOWER* negatively regulates ethylene response DNA-binding factors by activating an ethylene-responsive factor to control *Arabidopsis* floral organ senescence and abscission. *Plant Physiol.* **168**, 1666–1683 (2015).
- Chen, M. K., Lee, P. F. & Yang, C. H. Delay of flower senescence and abscission in *Arabidopsis* transformed with an *FOREVER YOUNG FLOWER* homolog from *Oncidium* orchid. *Plant Signal. Behav.* **6**, 1841–1843 (2011).
- Chen, W. H., Lee, Y. I. & Yang, C. H. Ectopic expression of two *FOREVER YOUNG FLOWER* Orthologues from *Cattleya* orchid suppresses ethylene signaling and *DELLA* results in delayed flower senescence/abscission and reduced flower organ elongation in *Arabidopsis*. *Plant Mol. Biol. Report.* **36**, 710–724 (2018).
- Chen, W. H., Jiang, Z. Y., Hsu, H. F. & Yang, C. H. Silencing of *FOREVER YOUNG FLOWER* like genes from *Phalaenopsis* orchids promotes flower senescence and abscission. *Plant Cell Physiol.* **62**, 111–124 (2021).
- Parenicová, L. et al. Molecular and phylogenetic analyses of the complete MADS-box transcription factor family in *Arabidopsis* new openings to the MADS world. *Plant Cell* **15**, 1538–1551 (2003).
- Ohno, S. *Evolution by Gene Duplication* (Springer-Verlag, 1970).
- Xu, G., Guo, C., Shan, H. & Kong, H. Divergence of duplicate genes in exon–intron structure. *Proc. Natl Acad. Sci. USA* **109**, 1187–1192 (2012).
- Kuzmin, E. et al. Exploring whole-genome duplicate gene retention with complex genetic interaction analysis. *Science* **368**, 1446 (2020).
- Cao, S. et al. Genetic architecture underlying light and temperature mediated flowering in *Arabidopsis*, rice, and temperate cereals. *N. Phytologist* **230**, 1731–1745 (2021).
- Gómez-Soto, D. et al. Overexpression of a *SOCI1*-related gene promotes bud break in *Ecodormant Poplars*. *Front. Plant Sci.* **12**, 670497 (2021).
- Lee, H. et al. The *AGAMOUS-LIKE 20* MADS domain protein integrates floral inductive pathways in *Arabidopsis*. *Genes Dev.* **14**, 2366–2376 (2000).
- Lee, J. & Lee, I. Regulation and function of *SOCI1*, a flowering pathway integrator. *J. Exp. Bot.* **61**, 2247–2254 (2010).
- Lee, S., Kim, J., Han, J. J., Han, M. J. & An, G. Functional analyses of the flowering time gene *OsMADS50*, the putative SUPPRESSOR OF OVEREXPRESSION OF CO 1/*AGAMOUS-LIKE 20* (*SOCI1/AGL20*) ortholog in rice. *Plant J.* **38**, 754–764 (2004).
- Preston, J. C., Jorgensen, S. A. & Jha, S. G. Functional characterization of duplicated SUPPRESSOR OF OVEREXPRESSION OF CONSTANS 1-Like genes in petunia. *PLOS ONE* **9**, e96108 (2014).
- Dorca-Fornell, C. et al. The *Arabidopsis* *SOCI1*-like genes *AGL42*, *AGL71*, and *AGL72* promote flowering in the shoot apical and axillary meristems. *Plant J.* **67**, 1006–1017 (2011).
- Schönrock, N. et al. Plycomb-group proteins repress the floral activator *AGL19* in the FLC-independent vernalization pathway. *Genes Dev.* **20**, 1667–1678 (2006).
- Liang, S. et al. Transcriptional regulations on the low-temperature-induced floral transition in an *Orchidaceae* species, *Dendrobium nobile*: An expressed sequence tags analysis. *Comp. Funct. Genomics* **2012**, 757801 (2012).
- Kim, W., Latrasse, D., Servet, C. & Zhou, D. X. *Arabidopsis* histone deacetylase *HDA9* regulates flowering time through repression of *AGL19*. *Biochem. Biophys. Res. Commun.* **432**, 394–398 (2013).
- Kang, M. J., Jin, H. S., Noh, Y. S. & Noh, B. Repression of flowering under a noninductive photoperiod by the *HDA9-AGL19-FT* module in *Arabidopsis*. *N. Phytol.* **206**, 281–294 (2015).

21. Liu, X. R. et al. Overexpression of an orchid (*Dendrobium nobile*) SOC1/TM3-Like ortholog, DnAGL19, in Arabidopsis regulates HOS1-FT expression. *Front. Plant Sci.* **7**, 99 (2016).
22. Pe' rez-Ruiz, R. V. et al. XAANTAL2 (AGL14) Is an important component of the complex gene regulatory network that underlies Arabidopsis shoot apical meristem transitions. *Mol. Plant.* **8**, 796–813 (2015).
23. Azpeitia, E. et al. Cauliflower fractal forms arise from perturbations of floral gene networks. *Science* **373**, 192–197 (2021).
24. Garay-Arroyo, A. et al. The MADS transcription factor XAL2/AGL14 modulates auxin transport during Arabidopsis root development by regulating PIN expression. *EMBO J.* **32**, 2884–2895 (2013).
25. Alvarez-Buylla, E. R. et al. MADS-box genes underground becoming mainstream: Plant root developmental mechanisms. *N. Phytol.* **223**, 1143–1158 (2019).
26. Xu, G., Huang, J., Lei, S. K., Sun, X. G. & Li, X. Comparative gene expression profile analysis of ovules provides insights into *Jatropha curcas* L. ovule development. *Sci. Rep.* **9**, 15973 (2019).
27. Force, A. et al. Preservation of duplicate genes by complementary, degenerative mutations. *Genetics* **151**, 1531–1545 (1999).
28. Semon, M. & Wolfe, K. H. Preferential subfunctionalization of slow-evolving genes after allopolyploidization in *Xenopus laevis*. *Proc. Natl Acad. Sci. USA* **105**, 8333–8338 (2008).
29. Cusack, B. P. & Wolfe, K. H. When gene marriages don't work out: Divorce by subfunctionalization. *Trends Genet.* **23**, 270–272 (2007).
30. Wapinski, I., Pfeffer, A., Friedman, N. & Regev, A. Natural history and evolutionary principles of gene duplication in fungi. *Nature* **449**, 54–61 (2007).
31. Butenko, M. A. et al. Inflorescence deficient in abscission controls floral organ abscission in Arabidopsis and identifies a novel family of putative ligands in plants. *Plant Cell* **15**, 2296–2307 (2003).
32. de Folter, S. et al. Comprehensive interaction map of the Arabidopsis MADS box transcription factors. *Plant Cell* **17**, 1424–1433 (2005).
33. Schauer, S. E. et al. Intronic regulatory elements determine the divergent expression patterns of AGAMOUS-LIKE6 subfamily members in Arabidopsis. *Plant J.* **59**, 987–1000 (2009).
34. Flanagan, C. A. & Ma, H. Spatially and temporally regulated expression of the MADS-box gene AGL2 in wild-type and mutant Arabidopsis flowers. *Plant Mol. Biol.* **26**, 581–595 (1994).
35. Rounsley, S. D., Ditta, G. S. & Yanofsky, M. F. Diverse roles for MADS box genes in Arabidopsis development. *Plant Cell* **7**, 1259–1269 (1995).
36. Hsu, H. F. et al. Model for perianth formation in orchids. *Nat. Plants* **1**, 15046 (2015).
37. Theissen, G. & Saedler, H. Plant biology. Floral quartets. *Nature* **409**, 469–471 (2001).
38. Fernandez, D. E. et al. The embryo MADS domain factor AGL15 acts postembryonically: Inhibition of perianth senescence and abscission via constitutive expression. *Plant Cell* **12**, 183–198 (2000).
39. Adamczyk, B. J., Lehti-Shiu, M. D. & Fernandez, D. E. The MADS domain factors AGL15 and AGL18 act redundantly as repressors of the floral transition in Arabidopsis. *Plant J.* **50**, 1007–1019 (2007).
40. Mao, W. T., Hsu, W. H., Li, J. Y. & Yang, C. H. Distance-based measurement determines the coexistence of B protein hetero- and homodimers in lily tepal and stamen tetrameric complexes. *Plant J.* **105**, 1357–1373 (2021).
41. Sieburth, L. E. & Meyerowitz, E. M. Molecular dissection of the AGAMOUS control region shows that cis elements for spatial regulation are located intragenically. *Plant Cell* **9**, 355–365 (1997).
42. Deyholos, M. K. & Sieburth, L. E. Separable whorl-specific expression and negative regulation by enhancer elements within the AGAMOUS second intron. *Plant Cell* **12**, 1799–1810 (2000).
43. Sheldon, C. C., Conn, A. B., Dennis, E. S. & Peacock, W. J. Different regulatory regions are required for the vernalization-induced repression of FLOWERING LOCUS C and for the epigenetic maintenance of repression. *Plant Cell* **14**, 2527–2537 (2002).
44. Kooiker, M. et al. BASIC PENTACYSTEINE1, a GA binding protein that induces conformational changes in the regulatory region of the homeotic Arabidopsis gene SEEDSTICK. *Plant Cell* **17**, 722–729 (2005).
45. Gu, R. et al. Functional Characterization of the promoter and second intron of CUM1 during flower development in cucumber (*Cucumis sativus* L.). *Horticultural. Plant J.* **4**, 103–110 (2018).
46. Chang, Y. Y. et al. Characterization of the possible roles for B class MADS box genes in regulation of perianth formation in orchid. *Plant Physiol.* **152**, 837–853 (2010).
47. Murashige, T. & Skoog, F. A revised medium for rapid growth and bioassays with tobacco tissue cultures. *Physiol. Plant* **15**, 473–479 (1962).
48. Clough, S. J. & Bent, A. F. Floral dip: A simplified method for *Agrobacterium*-mediated transformation of *Arabidopsis thaliana*. *Plant J.* **16**, 735–743 (1998).
49. Chou, M. L., Haung, M. D. & Yang, C. H. EMF interact with late-flowering genes in regulating floral initiation genes during shoot development in Arabidopsis. *Plant Cell Physiol.* **42**, 499–507 (2001).
50. Jefferson, R. A., Kavanagh, T. A. & Bevan, M. GUS fusions:  $\beta$ -glucuronidase as a sensitive and versatile gene fusion marker in higher plants. *EMBO J.* **6**, 3901–3907 (1987).
51. Chen, W. H., Hsu, W. H., Hsu, H. F. & Yang, C. H. A tetraspanin gene regulating auxin response and affecting orchid perianth size and various plant developmental processes. *Plant Direct* **3**, 1–20 (2019).
52. Chen, Q. G. & Bleecker, A. B. Analysis of ethylene signal-transduction kinetics associated with seedling-growth response and chitinase induction in wild-type and mutant Arabidopsis. *Plant Physiol.* **108**, 597–607 (1995).
53. Hsu, W. H. et al. AGAMOUS-LIKE13, a putative ancestor for the E functional genes, specifies male and female gametophyte morphogenesis. *Plant J.* **77**, 1–15 (2014).

## Acknowledgements

This work was supported by grants to C.-H.Y. from the Ministry of Science and Technology, Taiwan, ROC, grant number: MOST 107-2313-B-005-018-MY3 and MOST 109-2326-B-005-001. This work was also financially supported (in part) by the Advanced Plant Biotechnology Center from The Featured Areas Research Center Program within the framework of the Higher Education Sprout Project by the Ministry of Education (MOE) in Taiwan.

## Author contributions

C.-H.Y. developed the overall strategy, designed experiments, and coordinated the project. W.-H.C., P.-T.L., C.-W.T., and M.-C.H. generated transgenic Arabidopsis plants, performed phenotypic and gene expression analyses. H.-F.H. and Y.-C.L. performed gene expression analyses. W.-H.H., C.-W.T., P.-T.L., and W.-T.M. performed FRET analyses. C.-H.Y. prepared and revised the manuscript.

## Competing interests

The authors declare no competing interests.

## Additional information

**Supplementary information** The online version contains supplementary material available at <https://doi.org/10.1038/s42003-022-03629-w>.

**Correspondence** and requests for materials should be addressed to Chang-Hsien Yang.

**Peer review information** *Communications Biology* thanks Jazmin Abraham and the other anonymous reviewer(s) for their contribution to the peer review of this work. Primary Handling Editors: José Estevez and Luke R. Grinham.

**Reprints and permission information** is available at <http://www.nature.com/reprints>

**Publisher's note** Springer Nature remains neutral with regard to jurisdictional claims in published maps and institutional affiliations.



**Open Access** This article is licensed under a Creative Commons Attribution 4.0 International License, which permits use, sharing, adaptation, distribution and reproduction in any medium or format, as long as you give appropriate credit to the original author(s) and the source, provide a link to the Creative Commons license, and indicate if changes were made. The images or other third party material in this article are included in the article's Creative Commons license, unless indicated otherwise in a credit line to the material. If material is not included in the article's Creative Commons license and your intended use is not permitted by statutory regulation or exceeds the permitted use, you will need to obtain permission directly from the copyright holder. To view a copy of this license, visit <http://creativecommons.org/licenses/by/4.0/>.

© The Author(s) 2022